Young et al., "The response of Jakobshavn Isbræ to Holocene climate change" Data Repository item

^{10}Be dating

Samples from sculpted gneiss bedrock surfaces (*n* = 14) and perched erratics (*n* = 4) were collected with a hammer and chisel. Samples were collected from horizontal to near-horizontal surfaces and we avoided sampling from boulder edges and corners. Geographic coordinates and elevation for each sample were collected with a handheld GPS device, and a clinometer was used to measure shielding by surrounding topography for two samples (FST08-BR; FST08-04). Remaining samples did not require measurement of the surrounding topography. Samples were collected at elevations above the local marine limit, which is at least 80 m.a.s.l. near the outer coast and ~40 m.a.s.l. inboard of the Fjord Stade moraines (Long et al., 2006, Long and Roberts, 2002). Fjord Stade moraines adjacent to the Isfjord shown in figure 1 (main text) were initially mapped on aerial photographs and then checked in the field by walking their respective crests with a handheld GPS unit.

All samples were processed at the University at Buffalo Cosmogenic Isotope Laboratory following procedures modified from Kohl and Nishiizumi (1992). Samples were first crushed and sieved to isolate the 425-850 µm size fraction and then pretreated in dilute HCl and HNO_3-HF acid baths. Quartz was isolated by heavy-liquid mineral separation and additional HNO_3-HF heated sonification baths. ^{9}Be carrier (~0.25-0.45 mg) was added to each sample prior to dissolution in concentrated HF. Beryllium was extracted using ion-exchange chromatography, selective precipitation with NH_4OH, and final oxidation to BeO.

^{10}Be/^{9}Be AMS measurements were completed at the Lawrence Livermore National Laboratory Center for Mass Spectrometry and normalized to standard 07KNSTD3110 (Nushiizumi et al., 2007). Ratios for dissolution process blanks (*n* = 3) averaged $2.10\text{x}10^{-14}$ with a lowest achieved process blank ratio of $2.10\text{x}10^{-15}$. AMS precision for blank-corrected ^{10}Be/^{9}Be sample ratios ranged from 2.5-5.3%.

^{10}Be exposure ages (tables DR1, DR2) were calculated using the CRONUS-Earth online exposure age calculator (http://hess.ess.washington.edu/math; Version 2.2; Balco et al., 2008). As this region has undergone isostatic uplift since deglaciation, the measured sample elevation does not reflect the sample elevation history. Prior to calculating ^{10}Be exposure ages, sample elevation was corrected by using a minimum marine limit of 80 m asl, and a regional emergence curve spanning the last ~9.5 cal ka BP Long et al., 2006; Long and Roberts, 2002). We used isolation basin data from Long et al. (2006) and Long and Roberts (2002) to generate three separate emergence curves representing 1) emergence since ~9.5 cal ka BP for our most distal samples, 2) emergence since ~7.9 ka for samples located immediately inboard of the Tasiussaq moraine, and 3) emergence since ~7.4 cal ka BP for samples located just outboard of the LIA margin. Emergence data was plotted graphically, fit with a 3rd order polynomial trend line, and finally the trend line for each equation was solved. Emergence curve solutions provide the necessary elevation corrections needed for each sample. Resulting elevation corrections are -15.6 m for samples located outboard of the Fjord Stade (FS) moraines, -4.6 m for samples located immediately inboard of the FS moraines, and -0.2 m for samples located just beyond the LIA margin. We employed a regionally calibrated ^{10}Be production rate of 3.93±0.19 atoms g^{-1} yr^{-1} (i.e. Balco et al., 2009) and the constant-production scaling scheme of Lal/Stone (Lal, 1991; Stone, 2000), resulting in ^{10}Be exposure ages ~12% older than ages calculated using the globally-calibrated production rate of 4.49±0.43 atoms g^{-1} yr^{-1} (Balco et al., 2008). These values are lower than the production rates reported in Balco et al. (2008) and Balco et al. (2009) and reflect a recent update to the Be isotope ratio standard of Nishiizumi et al. (2007; 07KNSTD3110). Full documentation of this change is available at the aforementioned CRONUS-Earth website. As the influence of the earth's magnetic field on ^{10}Be production is negligible at the study area's relatively high latitude (~69ºN; Gosse and Phillips, 2001), all ^{10}Be exposure ages reported in the main text use the constant-production scheme of Lal/Stone (1991; 2000; table DR1). ^{10}Be ages using alternative scaling schemes (i.e. Lifton et al., 2005; Desilets and Zreda, 2003; Desilets et al., 2006; Dunai, 2001) that incorporate time-dependent production rates based on fluctuations in the earth's magnetic field are presented in table DR2. ^{10}Be ages calculated using these scaling schemes result in age differences that are minimal (<2%), and while different scaling schemes may alter absolute ^{10}Be ages, our relative chronology remains unchanged.

Both snow cover and erosion can lead to apparent ^{10}Be exposure ages that are younger than absolute ^{10}Be ages. Bedrock samples were collected from windswept locations (i.e. ridge crests) and all sampled boulders were at least 2.5 m tall. We observe no correlation between boulder height and ^{10}Be age, which would be expected with significant snow cover. We consider the effects of snow cover minimal and note that glacial polish and striations were routinely observed on both bedrock and boulder surfaces, indicating negligible erosion. Thus, presented ^{10}Be ages are not corrected for shielding by snow cover or erosion.

Sample FST08-BR, which yielded a ^{10}Be age of 12.0±0.3 ka was not included in our discussion and likely contains ^{10}Be inherited from a previous period of exposure. This sample is >2σ older than all remaining samples located just inside of the FS moraines and FST08-04, which was collected immediately adjacent to FST08-BR, has a ^{10}Be age of 8.1±0.3 ka. Moreover, sample FST08-BR is >2σ older than samples located outside of the FS moraines (10.2±0.1 ka; n = 5).

Lake sediment cores

Multiple sediment cores for this study were collected from two lakes (Fig. 2). Lake bathymetry was determined using a Garmin GPSMAP 400 series GPS receiver connected to a dual beam depth transducer. Sediment cores were collected using the Universal Coring system (Aquatic Research Instruments; www.aquaticresearch.com) with 5-cm-diameter polycarbonate core tubes; sediment cores were recovered with intact sediment-water interfaces, which were allowed to dewater for several days prior to being packaged for transport to the University at Buffalo. In the lab, cores were split lengthwise, photographed and logged. Magnetic susceptibility (MS) was measured every 0.5 cm using a Bartington MS2E High Resolution Surface Scanning Sensor scanner connected to a Bartington MS2 Magnetic Susceptibility Meter. Organic matter content was measured every 0.5 cm using the loss-on-ignition (LOI) procedure at 550°C. Multiple sediment cores were obtained from Iceboom lake, which has a complex bathymetry and several different sub-basins; cores were collected from the deepest point in two sub-basins on the opposite side of the lake from the inflow sources. 08ICE-3 is 99 cm long and was collected at 12.21 m depth (69°13’58” N, 50°35’00” W); 08ICE-5 is 76 cm long and was collected at 3.12 m water depth (69°14’8” N, 50°1’7” W). The general stratigraphy, MS and LOI data are shown in figure 2. A sediment core was also collected from small lake 300 m north of Iceboom Lake’s outflow that has not been connected to the ice sheet drainage network since deglaciation. 08NOR-3 is 106 cm long and was collected at 3.85 m water depth (69°14'29.82"N, 50° 1'38.01"W). The bottom 2 cm in the core comprise organic-poor sand, which is overlain by organic rich lake sediment.

Pieces of aquatic moss were picked for ^{14}C dating from two intervals in 08ICE-3, four intervals in 08ICE-5, and three intervals in 08NOR-3 (Table DR4). After being washed with deionized water at the University at Buffalo, cleaned samples were subsequently prepared at the INSTAAR Laboratory for AMS Radiocarbon Preparation and Research at the University of Colorado and measured at the W.M. Keck Carbon Cycle AMS Facility at the University of California, Irvine. Radiocarbon ages were calibrated with CALIB v 6.0 (http://radiocarbon.pa.qub.acuk/calib/; Stuiver et al., 2010) and the IntCal09 calibration curve (Reimer et al., 2009).

The basal radiocarbon age from 08ICE-5 and the ^{10}Be ages for deglaciation match well. However, the basal radiocarbon age from 08NOR-3 is ~500 yr older than both the basal radiocarbon age from 08ICE-5 and the ^{10}Be ages for deglaciation near the Neoglacial maximum ice margin. Additionally, the $\delta^{13}C$ value of the macrofossils that were dated is atypical of all other macrofossils dated from lakes in this region, implying a complicated carbon pool in the lake. Furthermore, a marine influence on the $\delta^{13}C$ value is highly unlikely as North Lake rests at ~180 m.a.s.l., well above the local marine limit (~40 m.a.s.l.). In any case, because the majority of the geochronology suggests deglaciation of NOR and ICE lakes occurred ~7.4 ka, we use 7400 cal yr BP for the initiation of organic matter deposition in 08NOR-3. Our temperature reconstruction presented in figure 3 (main text) depicts the onset of organic sedimentation at 7.4 ka.

Chironomids

Chironomids (non-biting midges, Diptera: Chironomidae) were analyzed at 13 depths in the 08NOR-3 sediment core (Figs. 3, DR1) and in a surface sediment sample collected from the same lake in 2009. Sediment samples were deflocculated with warm 5% KOH for 20 minutes and rinsed on a 100µm mesh sieve. Head capsules were manually picked from a Bogorov sorting tray under a 40x power dissecting microscope, then permanently mounted on slides using Euparal. All samples contained at least 50 whole identifiable head capsules, and 11 different fossil taxa were enumerated. Chironomids were analyzed according to standard protocol (e.g. Walker, 2001) and taxonomic identifications followed Brooks et al. (2007) with reference to Oliver and Roussel (1983) and Wiederholm (1983), and taxa were lumped to harmonize with Francis et al. (2006).

July air temperatures were modeled using a chironomid-temperature transfer function developed for northeastern North America, which includes training set (calibration) sites in the Eastern Canadian Arctic west of Greenland (Francis et al., 2006; Walker et al., 1997). The weighted-averaging regression model uses square-root transformed species data and has a root mean squared error of prediction (RMSEP) of 1.5°C for mean July air temperatures. This transfer function has previously been used to reconstruct Holocene paleotemperatures at a lake in west Greenland (e.g. Wooller et al., 2004), as well as numerous lakes in the Canadian Arctic (Axford et al., 2009; Francis et al., 2006; Briner et al., 2006). Paleotemperatures were modeled using the software program C2 v 1.4.3 (Juggins, 2003), and are expressed as anomalies (in °C) relative to the modern estimate from North Lake surface sediments (Figs. 3, DR1). The applicability of the transfer function to the fossil data was assessed by two means: One, it was noted that all fossil taxa were represented in the training set (*Tanytarsus lugens* type and *Micropsectra* type are lumped within Tanytarsini undiff. for the temperature modeling); and two, the statistical software package R v 2.2.1 was used to calculate the squared-chord distance (SCD) between each downcore assemblage and its closest analog in the training set. For all but one sample, SCD <0.5; the remaining sample has SCD 0.74 from its closest analog in the training set (Fig. DR1).

CAPTION FOR FIGURE DR1:

Figure DR1. Downcore data from sediment core 08-NOR-3, including chronology, head capsule concentrations, chironomid species percentages, squared-chord distance (SCD) of each sample from its closest analog in the training set, and chironomid-inferred July air temperatures (expressed as differences from the modern estimate obtained from chironomids in surface sediments). The age-depth model consists of three radiocarbon dates and an additional point at the surface representing present day. Arrow points to the likely onset of organic sedimentation (~7.4 ka) derived from nearby ^{10}Be ages and the basal radiocarbon age from Iceboom Lake.

Supplemental References:

Balco, G., Stone, J.O., Lifton, N.A., and Dunai, T.J., 2008, A complete and easily accessible means of calculating surface exposure ages or erosion rates from ^{10}Be and ^{26}Al measurements: Quateranry Geochronology, v. 3, p. 174-195.

Balco, G., Briner, J., Finkel, R.C., Rayburn, J.A., Ridge, J.C., and Schaefer, J.M., 2009, Regional beryllium-10 production rate calibration for northeastern North America: Quaternary Geochronology, v. 4, p. 93-107.

Briner, J.P., Michelutti, N., Francis, D.R., Miller, G.H., Axford, Y., Woller, M.J., and Wolfe, A.P., 2006, A multi-proxy lacustrine record of Holocene climate change on northeastern Baffin Island, Arctic Canada: Quaternary Research, v. 65, 431-442.

Brooks, S.J., Langdon, P.G. and Heiri, O., 2007, The identification and use of Palaearctic Chironomidae larvae in palaeoecology. QRA Technical Guide 10, Quaternary Research Association, London. 276 p.

Desilets, D., and Zreda, M., 2003, Spatial and temporal distribution of secondary cosmic ray nucleon intensities and applications to in-situ cosmogenic dating: Earth and Planetary Science Letters, v. 206, p. 21–42.

Desilets, D., Zreda, M., and Prabu, T., 2006, Extended scaling factors for in situ cosmogenic nuclides: New measurements at low latitude: Earth and Planetary Science Letters, v. 246, p. 265-276.

Dunai, T.J., 2001, Influence of secular variation of the magnetic field on production rates of in situ produced cosmogenic nuclides: Earth and Planetary Science Letters, v. 193, p. 197-212.

Francis, D.R., Wolfe, A.P., Walker, I.R., and Miller, G.H., 2006, Interglacial and Holocene temperature reconstructions based on midge remains in sediments of two lakes from Baffin Island, Nunavut, Arctic Canada: Palaeogeography, Palaeoclimatology, Palaeoecology, v. 236, p. 107–124.

Gosse, J.C., and Phillips, F.M., 2001, Terrestrial in situ cosmogenic nuclides: theory and application: Quaternary Science Reviews, v. 20, p. 1475–1560.

Juggins, S., 2003, C2 User guide. Software for ecological and palaeoecological data analysis and visualization. University of Newcastle, Newcastle upon Tyne, UK. 69 p.

Kohl, C.P. and Nishiizumi, K., 1992. Chemical isolation of quartz for measurement of in situ- produced cosmogenic nuclides: Geochimica Cosmochimica Acta, v. 56, p. 3583–3587.

Lal, D., 1991, Cosmic ray labeling of erosion surfaces: *in situ* nuclide production rates and erosion models: Earth and Planetary Science Letters, v. 104, p. 424-439.

Lifton, N.A., Beiber, J.W., Clem, J.M., Duldig, M.L., Evenson, P., Humble, J.E., and Pyle, R., 2005, Addressing solar modulation and long-term uncertainties in scaling secondary cosmic rays for in situ cosmogenic nuclide applications: Earth and Planetary Science Letters, v. 239, p. 140-161.

Long, A.J., Roberts, D.H., and Dawson, S., 2006, Early Holocene history of the west Greenland Ice Sheet and the GH-8.2 event: Quaternary Science Reviews, v. 25, p. 904-922.

Nishiizumi, K., Imamura, M., Caffee, M., Southon, J., Finkel, R., and McAnich, J., 2007, Absolute calibration of 10Be AMS standards: Nuclear Instruments and Methods in Physics Research B, v. 258, p. 403-413.

Oliver, D.R., and Roussel, M.E., 1983, The Insects and Arachnids of Canada: Part 11. The Genera of Midges of Canada; Diptera: Chironomidae 1746, Agriculture Canada, Ottawa.

Reimer, P.J., Baillie, M.G.L., Bard, E., Bayliss, A., Beck, J.W., Blackwell, P.G., Bronk Ramsey, C., Buck, C.E., Burr, G.S., Edwards, R.L., Friedrich, M., Grootes, P.M., Guilderson, T.M., Hajdas, I., Heaton, T.J., Hogg, A.G., Hughen, K.A., Kaiser, K.F., Kromer, B., McCormac, F.G., Manning, S.W., Reimer, R.W., Richards, D.A., Southon, J.R., Talamo, S., Turney, C.S.M., van der plicht, J., and Weyhenmeyer, C.E., 2009, IntCal09 and Marine09 Radiocarbon Age Calibration Curves, 0–50,000 Years cal BP: Radiocarbon, v. 51, p. 1111-1150.

Stone, J.O., 2000, Air pressure and cosmogenic isotope production: Journal of Geophysical Research, v. 105, p. 23753–23759.

Stuiver, M., Reimer, P. J. and Reimer, R. W., 2010, CALIB 6.0. WWW program and documentation. Available at http://calib.qub.ac.uk/calib/.

Walker, I.R., in Tracking Environmental Change Using Lake Sediments, eds Smol, J.P., Birks, H.J.B., and Last, W.M., 2001, Kluwer, Dordrecht, The Netherlands) 4, 43-66.

Walker, I.R., Levesque, J., Cwynar, L.C. and Lotter, A.F., 1997, An expanded surface-water paleotemperature inference model for use with fossil midges from eastern Canada: Journal of Paleolimnology, v. 18, p. 165-178.

Weidick, A., 1972, C^{14} dating of survey material performed in 1971: Rapport Grønlands Geologiske Undersøgelse. v. 45, p. 58-67.

Weidick, A., and Bennike, O., 2007, Quaternary glaciation history and glaciology of Jakobshavn Isbræ and the Disko Bugt region, West Greenland: a review: Geological Survey of Denmark and Greenland Bulletin 14, 78 p.

Wiederholm, T. (Ed.), 1983, Chironomidae of the Holarctic Region. Keys and Diagnoses: Part 1. Larvae. Entomoogical Scandinivica Supplement 19, pp. 457.

Wooller, M.J., Franics, D., Fogel, M.L., Miller, G.F., Walker, I.R., Wolfe, A.P., 2004, Quantitative paleotemperature estimates from d18O of chironomid head capsules preserved in arctic lake sediments: Journal of Paleolimnology v, 31, p. 267-274.

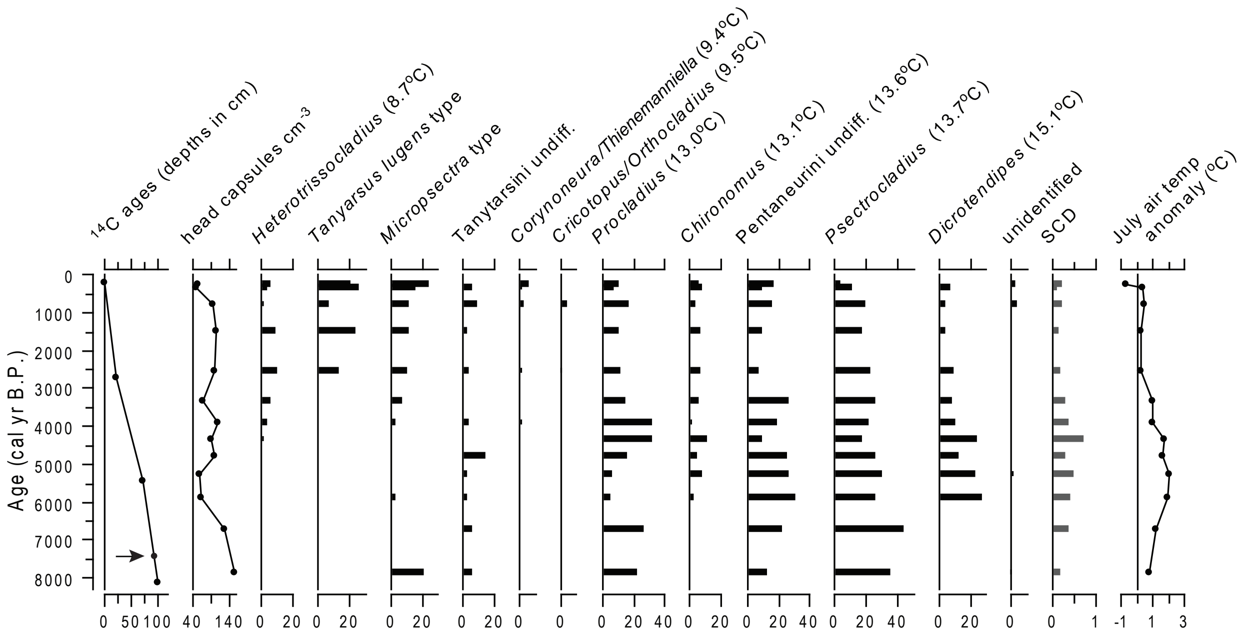

Figure DR1 (Supplementary Figure)

Table DR1: ^{10}Be sample information for Jakobshavn Isbræ

Sample	Latitude (N)	Longitude (W)	Elevation (m asl)	Corrected elevation (m asl)[a]	Sample height (m)	Thickness (cm)	Shielding correction	Quartz (g)	Be carrier added (g)[b]	^{10}Be (atoms g^{-1})	^{10}Be uncertainty (atoms g^{-1})	^{10}Be age[c]
Outboard of Fjord Stade moraines												
JAKN08-01	69° 12.331'	51° 07.465'	112	96	0	2.5	1.000	80.0463	0.4480	47575.8166	1168.264	10.2 ± 0.2
JAKN08-08	69° 11.958'	50° 58.043'	338	322	0	1.0	1.000	85.0596	0.2969	61424.170	1727.041	10.3 ± 0.3
JAKN08-21	69° 14.594'	50° 58.842'	390	374	0	1.0	1.000	75.4874	0.3800	63882.262	3382.958	10.2 ± 0.5
JAKN08-22	69° 14.459'	50° 57.683'	360	344	3.0	4.5	1.000	80.1615	0.3930	59644.6241	1868.383	10.1 ± 0.3
09GRO-01	69° 06.590'	51° 02.487'	204	188	0	5.0	1.000	77.0936	0.2514	50245.693	1253.572	10.0 ± 0.2
Inboard of Fjord Stade moraines												
JAKN08-13	69° 11.065'	50° 54.359'	180	175	0	2.5	1.000	80.1692	0.4570	41081.8675	1042.701	8.1 ± 0.2
FST08-BR	69° 11.844'	51° 03.244'	65	60	0	2.0	0.999	80.0250	0.2513	53768.095	1337.201	12.0 ± 0.3
FST08-04	69° 08.792'	51° 03.225'	65	60	2.5	2.0	0.999	80.3201	0.2511	36283.838	940.838	8.1 ± 0.2
09GRO-03	69° 06.820'	51° 03.858'	124	119	0	3.0	1.000	76.7977	0.2512	38918.931	1139.028	8.1 ± 0.2
09GRO-06	69° 06.970'	50° 59.467'	245	240	2.5	4.5	1.000	74.5675	0.2515	41475.243	1323.184	7.8 ± 0.2
09GRO-33	69° 11.469'	51° 00.441'	125	120	2.5	4.5	1.000	76.0270	0.2517	37484.239	1168.586	8.0 ± 0.2
Little Ice Age margin												
JAKN08-28	69° 14.444'	49° 59.109'	215	215	0	1.0	1.000	85.0930	0.3015	39588.0588	1902.308	7.4 ± 0.4
JAKN08-39	69° 13.283'	49° 59.712'	206	206	0	3.0	1.000	85.3685	0.2988	38695.1865	1261.777	7.4 ± 0.2
JAKN08-40	69° 13.536'	50° 03.411'	147	147	0	2.0	1.000	80.0340	0.4563	38904.9208	996.522	7.9 ± 0.2
JAKN08-44	69° 18.465'	50° 08.873'	347	347	0	2.0	1.000	80.2219	0.4103	44534.0809	1675.958	7.3 ± 0.3
JAKN08-56	69° 18.030'	50° 19.723'	425	425	0	1.0	1.000	80.0070	0.4539	49360.0035	1214.232	7.5 ± 0.2
JAKS08-33	69° 08.823'	50° 07.471'	222	222	0	1.0	1.000	80.2910	0.4062	40672.5553	1726.658	7.5 ± 0.3
JAKS08-34	69° 08.792'	50° 06.220'	180	180	0	2.0	1.000	80.1042	0.4540	38012.879	975.175	7.4 ± 0.2

[a]Sample elevation was corrected using a regional emergence curve with a marine limit of 80 m asl; elevations have been rounded to the nearest m

[b]All samples were spiked with a 405µg/g ^{9}Be carrier and AMS results are standardized to 07KNSTD3110

[c]Be ages given in ka at 1SD using the scaling scheme of Lal (1991)/Stone (2000). Comaparison with other scaling schemes are shown in Table S2

Table DR2: ^{10}Be ages using alternative scaling schemes

Sample	St	De	Du	Li	Lm
Outboard of Fjord Stade moraines					
JAKN08-01	10.2 ± 0.2	10.0 ± 0.2	9.9 ± 0.2	9.8 ± 0.2	10.4 ± 0.2
JAKN08-08	10.3 ± 0.3	10.3 ± 0.3	10.1 ± 0.3	10.1 ± 0.3	10.5 ± 0.3
JAKN08-21	10.2 ± 0.5	10.2 ± 0.5	10.0 ± 0.5	9.9 ± 0.5	10.3 ± 0.5
JAKN08-22	10.1 ± 0.3	10.1 ± 0.3	9.9 ± 0.3	9.8 ± 0.3	10.2 ± 0.3
09GRO-01	10.0 ± 0.2	9.9 ± 0.2	9.7 ± 0.2	9.7 ± 0.2	10.1 ± 0.2
Inboard of Fjord Stade moraines					
JAKN08-13	8.1 ± 0.2	8.0 ± 0.2	7.9 ± 0.2	7.8 ± 0.2	8.2 ± 0.2
FST08-BR	12.0 ± 0.3	11.7 ± 0.3	11.5 ± 0.3	11.5 ± 0.3	12.1 ± 0.3
FST08-04	8.1 ± 0.2	7.9 ± 0.2	7.7 ± 0.2	7.7 ± 0.2	8.2 ± 0.2
09GRO-03	8.1 ± 0.2	8.0 ± 0.2	7.9 ± 0.2	7.9 ± 0.2	8.3 ± 0.2
09GRO-06	7.8 ± 0.2	7.7 ± 0.2	7.6 ± 0.2	7.5 ± 0.2	7.9 ± 0.2
09GRO-33	8.0 ± 0.2	7.8 ± 0.2	7.7 ± 0.2	7.6 ± 0.2	8.1 ± 0.2
Little Ice Age margin					
JAKN08-28	7.4 ± 0.4	7.3 ± 0.2	7.2 ± 0.2	7.2 ± 0.2	7.5 ± 0.2
JAKN08-39	7.4 ± 0.2	7.4 ± 0.3	7.2 ± 0.3	7.2 ± 0.3	7.5 ± 0.3
JAKN08-40	7.9 ± 0.2	7.8 ± 0.2	7.7 ± 0.2	7.6 ± 0.2	8.0 ± 0.2
JAKN08-44	7.3 ± 0.3	7.3 ± 0.2	7.2 ± 0.2	7.2 ± 0.2	7.5 ± 0.2
JAKN08-56	7.5 ± 0.2	7.5 ± 0.2	7.4 ± 0.2	7.3 ± 0.2	7.6 ± 0.2
JAKS08-33	7.5 ± 0.3	7.5 ± 0.3	7.4 ± 0.3	7.3 ± 0.3	7.7 ± 0.3
JAKS08-34	7.4 ± 0.2	7.3 ± 0.2	7.2 ± 0.2	7.2 ± 0.2	7.5 ± 0.2

^{10}Be exposure ages calcuated using a regionally calibrated North American production rate (Balco et al., 2009) and five scaling schemes: *St,* (Lal, 1991, and Stone 2000) from table DR1; *De* (Desilets and others, 2003, 2006); *Du* (Dunai, 2001); *Li* (Lifton et al., 2005); and *Lm* (Lal, 1991 and Stone 2000 - time dependent)

Table DR3: Preexisting radiocarbon information

Latitude N	Longtitude W	Material Dated	Radiocarbon Age (^{14}C yr BP)	Calibrated Age (cal yr BP ± 2σ)	δ^{13}C (‰PDB)	Lab Number	Reference
Deglaciation of Isfjord							
69º12′	51º04′	*Macoma calcarea* shell	8795±130	9470±350[a]	0	Ua-1086	Weidick and Bennike, 2007
69º06′	51º04′	shells	8630±130	9787±366	NA	K-1818	Weidick, 1972
69º07′	50º37′	bulk sediment	6750±40	7599±75	-21.4	Beta-178169	Long et al., 2006
68º07′	50º35′	bulk sediment	6910±40	7767±96	-20.5	Beta-178170	Long et al., 2006
69º07′	50º38′	bulk sediment	7960±40	8819±172	-20.7	Beta-178168	Long et al., 2006
Reworked marine fauna in historic moraine							
68º06′	50º02′	*Mya truncata* shell	3590±65	3492±156[a]	1.88	Ua-4581	Weidick and Bennike, 2007
68º06′	50º02′	*Hiatella artica* shell	3940±65	3935±190[a]	1.92	Ua-4582	Weidick and Bennike, 2007
68º06′	50º02′	*Mya truncata* shell	3945±70	3933±204[a]	2.50	Ua-4580	Weidick and Bennike, 2007
68º06′	50º02′	*Mya truncata* shell	4075±70	4123±214[a]	2.16	Ua-4583	Weidick and Bennike, 2007
68º06′	50º02′	*Odobenus rosmarus* tusk	4290±100	4441±322[a]	-13.05	Ua-2350	Weidick and Bennike, 2007
68º06′	50º02′	*Mya truncata* shell	5240±75	5614±178[a]	1.85	Ua-4579	Weidick and Bennike, 2007
68º06′	50º02′	*Balanus* sp.plate	5710±55	6118±140[a]	0.98	Ua-4578	Weidick and Bennike, 2007

All samples were recalibrated using Calib 6.0 which utilizes the updated INTCAL09 dataset

[a] Corrected for a marine resevoir effect of 400 years

Table DR4: Radiocarbon sample information

Core	Depth (cm)	Material Dated	Fraction Modern	Radiocarbon Age (^{14}C yr BP)	Calibrated Age (cal yr BP ± 2σ)	$\delta^{13}C$ (‰PDB)	Lab Number
09-ICE-5	23	aquatic macrofossil	0.9591±0.0015	335±15	390±80	-23.5	CURL-10083
09-ICE-5	36	aquatic macrofossil	0.7952±0.0019	1840±20	1770±60	-27.8	CURL-10439
09-ICE-5	57	aquatic macrofossil	0.6098±0.0015	3980±20	4470±50	-30.7	CURL-10434
09-ICE-5	70	aquatic macrofossil	0.4534±0.0013	6360±25	7300±120	-30.5	CURL-10441
09-ICE-3	45	aquatic macrofossil	0.9370±0.0013	525±15	530±20	-22.4	CURL-10081
09-ICE-3	95	aquatic macrofossil	0.5119±0.0009	5380±15	6200±80	-28.4	CURL-10093
09-NOR-3	23	aquatic macrofossil	0.7265±0.0010	2565±15	2680±60	-28.1	CURL-10089
09-NOR-3	74	aquatic macrofossil	0.5562±0.0010	4715±20	5450±130	-28.6	CURL-10091
09-NOR-3	103	aquatic macrofossil	0.4006±0.0008	7350±20	8160±120	-12.7	CURL-10092